



Quantitative proteomics of auditory fear conditioning

Ingie Hong^{a,1}, Taewook Kang^{b,c,1}, Ki Na Yun^c, YongCheol Yoo^c, Sungmo Park^a, Jihye Kim^a, Bobae An^a, Sukwoon Song^a, Sukwon Lee^a, Jeongyeon Kim^a, Beomjong Song^a, Kyung-Hoon Kwon^c, Jin Young Kim^{c,*}, Young Mok Park^{b,c,*}, Sukwoo Choi^{a,*}

^a School of Biological Sciences, College of Natural Sciences, Seoul National University, Seoul 151-742, South Korea

^b Graduate School of Analytical Science and Technology (GRAT), Chungnam National University, Daejeon 305-333, South Korea

^c Mass Spectrometry Research Center, Korea Basic Science Institute, Ochang 363-883, South Korea

ARTICLE INFO

Article history:

Received 19 March 2013

Available online 28 March 2013

Keywords:

Auditory fear conditioning

Quantitative proteomics

TMT labeling

Lateral amygdala

Long-term potentiation

ABSTRACT

Auditory fear conditioning is a well-characterized rodent learning model where a neutral auditory cue is paired with an aversive outcome to induce associative fear memory. The storage of long-term auditory fear memory requires long-term potentiation (LTP) in the lateral amygdala and *de novo* protein synthesis. Although many studies focused on individual proteins have shown their contribution to LTP and fear conditioning, non-biased genome-wide studies have only recently been possible with microarrays, which nevertheless fall short of measuring changes at the level of proteins. Here we employed quantitative proteomics to examine the expression of hundreds of proteins in the lateral amygdala in response to auditory fear conditioning. We found that various proteins previously implicated in LTP, learning and axon/dendrite growth were regulated by fear conditioning. A substantial number of proteins that were regulated by fear conditioning have not yet been studied specifically in learning or synaptic plasticity.

© 2013 Elsevier Inc. All rights reserved.

1. Introduction

Learning and memory involve intricate molecular mechanisms in the brain at the transcriptional, translational, and post-translational level [1]. Whereas short-term memory does not require translation, long-term memory persists for hours to years and is known to require *de novo* protein synthesis [2]. This protein-synthesis dependent stabilization of memory into an enduring engram is called cellular consolidation [3]. A particularly well characterized learning paradigm is auditory-cued fear conditioning, which largely depends on the lateral amygdala (LA) [4–7]. Lateral amygdala input synapses are known to undergo long-term potentiation (LTP) upon fear conditioning [8,9], and this synaptic potentiation is crucial for learning the association between a neutral cue and an aversive outcome [10–12].

Which proteins are important in supporting the long-term memory engram? Although many studies focused on individual proteins have shown their contribution to synaptic plasticity and memory, non-biased genome-wide studies have only begun with the development of microarrays. Fear conditioning has also been studied through microarrays [13–15], but while microarray data

provide a genome-wide profile of gene expression, it still falls short of measuring translational and post-translational changes.

Mass spectrometry-based proteomics has single amino-acid sequence level resolution and offers an unprecedented detail in the biochemical assessment of biological processes. The breakthroughs in quantitative proteomics have largely accelerated research on proteome-wide network changes and the identification of previously unknown molecules [16–18]. Isobaric tags such as TMT and iTRAQ have enabled the comparison of expression levels of thousands of proteins across complex samples.

Here we use TMT tagging to explore proteome-wide changes upon associative learning. We employ the rat auditory fear conditioning model and compare protein expression in the lateral amygdala of naïve and fear conditioned animals. Unpaired controls, which received auditory cues and aversive footshock identical to the conditioned rats in an incongruous manner to prevent association, were used to discern changes that were specific to associative learning. Our results represent a quantitative proteomic approach to reveal the underlying translational mechanisms of auditory fear memory.

2. Materials and methods

2.1. Experimental animals

Male Sprague–Dawley rats (3–5 weeks old) were obtained from Orient Bio Inc. (Seongnam, Republic of Korea). Rats were housed in

* Corresponding author.

E-mail addresses: jinyoung@kbsi.re.kr (J.Y. Kim), ympark@kbsi.re.kr (Y.M. Park), sukwoo12@snu.ac.kr (S. Choi).

¹ These authors contributed equally to this work.

plastic cages and fed *ad libitum* under an inverted 12/12 light/dark cycle (light off at 9:00 AM). Behavioral training was done during the dark portion of the light/dark cycle. All behavioral procedures were approved by Institute of Laboratory Animal Resources of Seoul National University. All efforts were made to minimize animal suffering and to reduce the number of animals used.

2.2. Fear conditioning

For fear conditioning, rats were placed in a Plexiglas conditioning chamber and left undisturbed for 2 min [19–22]. A neutral tone (CS; 30 s, 2.8 kHz, 85 dB) co-terminating with an electrical foot shock (US; 1.0 mA, 1 s) was then presented three times with an average interval of 100 s. Rats were returned to their home cages 60 s after the last shock was applied. Twenty-four hours after conditioning, a subgroup of rats was presented with a tone (30 s, 2.8 kHz, 85 dB) in a distinct context to test memory retention. A separate subgroup of animals (18 in total: 6 rats per group without pooling) was used for proteomic analysis.

2.3. Slice preparation and sample preparation

Rats were anesthetized with isoflurane and decapitated to remove the brain as previously described [19]. The isolated whole brains were placed in an ice-cold modified aCSF solution containing (in mM) 175 sucrose, 20 NaCl, 3.5 KCl, 1.25 NaH_2PO_4 , 26 NaHCO_3 , 1.3 MgCl_2 and 11 D-(+)-glucose. Solutions were gassed with 95% O_2 /5% CO_2 . Coronal slices (400 μm) including the lateral amygdala were cut using a vibroslicer (NVSL, World Precision Instruments, Sarasota, FL) and the lateral amygdala was dissected and frozen immediately. Lateral amygdala tissue samples were homogenized in ice-cold modified RIPA buffer containing 50 mM Tris (pH 7.6), 150 mM NaCl, 5 mM NaF, 1 mM Na_3VO_4 , 0.5% Triton X-100, 0.5% sodium deoxycholate, 0.1% SDS and protease/phosphatase inhibitor cocktail. Samples were sonicated, boiled for 10 min, and spun down at 15,000g at 4 °C for 15 min. Protein content was quantified by a bicinchoninic acid assay (Thermo Scientific) following the manufacturer's protocol, and confirmed by SDS-PAGE and silver staining.

2.4. TMT labeling

Samples were subsequently tagged with tandem mass tags for quantitative mass spectrometry (TMTsixplex™ Isobaric Mass Tagging Kit, Thermo Scientific). Briefly, 100 μg of protein was taken from each sample and was reduced with 500 mM tris(2-carboxyethyl)phosphine (TCEP) at 55 °C for 1 h and then alkylated with 300 mM iodoacetamide (IAA) at 37 °C in the dark for 30 min. The samples were desalted using a 10,000 MW-cutoff membrane filter and dissolved in 100 mM triethylammonium bicarbonate (TEAB) buffer to a final concentration of 1 $\mu\text{g}/\mu\text{l}$. Sequencing grade trypsin (Promega, Madison, WI, USA) was added at 1:100 (w/w) into proteins in TEAB buffer and incubated overnight at 37 °C. The eighteen samples (six samples per group) were individually labeled using TMT-126, 129 (naïve controls), TMT-127, 130 (unpaired controls) and TMT-128, 131 (fear conditioned group) following the manufacturer's instructions. Aqueous hydroxylamine solution (5% w/v) was added to quench the reaction. Two samples from the three groups (6 samples) were then combined into 6-plex solutions for comparison, speed-vacuum dried, and then dissolved in 50 μl of water containing 0.1% formic acid for LC-MS/MS analysis. Finally, three batches of TMT-6-plex labeled peptides were prepared to compare a total of six samples per group ($n = 6$).

2.5. 2D-LC-MS/MS

The TMT-labeled samples were analyzed using a 2D-LC-MS/MS system consisting of a nanoACQUITY UltraPerformance LC System (Waters, USA) and a LTQ Orbitrap Elite mass spectrometer (Thermo Scientific, USA) equipped with a nano-electrospray source. A detailed description of 2D-LC-MS/MS analysis can be found in previous literatures [23,24]. Briefly, a strong cation exchange (5 μm , 3 cm) column was placed just before the C_{18} trap column (id 180 μm , length 20 mm, and particle size 5 μm ; Waters). Peptide solutions were loaded in 5 μl aliquots for each run. Peptides were displaced from the strong cation exchange phase to the C_{18} phase by a salt gradient that was introduced through an autosampler loop and then desalted for 10 min at a flow rate of 4 $\mu\text{l}/\text{min}$. Then, the trapped peptides were separated on a 200 mm homemade microcapillary column consisting of C_{18} (Aqua; particle size 3 μm) packed into 100 μm silica tubing with an orifice id of 5 μm .

An eleven-step salt gradient was performed using 3 μl of 0, 25, 50, 100, 250, and 500 mM ammonium acetate (0.1% formic acid in water) and 4, 5, 9 and an additional 9 μl at 500 mM ammonium acetate (0.1% formic acid in 30% ammonium acetate). The mobile phases, A and B, were composed of 0% and 100% acetonitrile, respectively, and each contained 0.1% formic acid. The LC gradient began with 5% B for 1 min and was ramped to 20% B over 5 min, to 35% B over 90 min, to 95% B over 1 min, and remained at 95% B over 13 min and 5% B for another 5 min. The column was re-equilibrated with 5% B for 15 min before the next run. The voltage applied to produce an electrospray was 2.0 kV. During the chromatographic separation, the LTQ Orbitrap Elite was operated in a data-dependent mode. The MS data were acquired using the following parameters: four data-dependent CID-high energy collision dissociation (CID-HCD) dual MS/MS scans per full scan; CID scans were acquired in LTQ with two-microscan averaging; full scans and HCD scans were acquired in Orbitrap at resolution 60,000 and 15,000, respectively, with two-microscan averaging; 35% normalized collision energy in CID and 45% normalized collision energy in HCD; ± 1 Da isolation window. Previously fragmented ions were excluded for 60 s. In CID-HCD dual scan, each selected parent ion was first fragmented by CID and then by HCD.

2.6. Protein identification, quantification, and statistical analysis

Probability-based (and error-tolerant) protein database searching of MS/MS spectra against the latest IPI rat protein database (IPI rat v3.70) was performed with a local MASCOT server (2.3, Matrix Science, London, UK) to identify and quantify proteins. The rate of decoy hits in the combined forward and reversed database was less than 1% of the forward hits on both the peptide and the protein levels in each of these experiments. Search criteria were set at: 20 ppm precursor ion mass tolerance, 0.5 Da product ion mass tolerance, two missed cleavages, trypsin as enzyme, TMT modification at the N-terminus and lysine residues and carbamidomethylation at cysteine residues as static modifications, oxidation at methionine, phosphorylation at serine, threonine, and tyrosine as a variable modifications, an ion score threshold of 20 and TMT-6-plex for quantification. Quantification was based on the averaged signal-to-noise ratio of TMT reporter product ions of more than two unique peptides.

Only the 482 proteins identified and quantified across all three TMT experiments were analyzed. The resulting ratios were logarithmized (base = 2) in order to achieve a normal distribution. Median and standard deviation were calculated, and ratio values corrected for the median to account for variability among different pairs [25]. Ratios were averaged and proteins with ratio values beyond $p < 0.05$ in normal distribution were defined as significantly regulated.

2.7. Gene annotation enrichment analysis

Gene Ontology annotation enrichment analysis was performed using the DAVID Bioinformatics Resource (v6.7) developed by the NIAID, National Institutes of Health [26]. DAVID analysis enabled the enrichment of functional-related gene groups and cellular compartments. Ingenuity Pathway Analysis (IPA; Ingenuity Systems, <http://www.ingenuity.com>) was used to functionally annotate genes implicated in known biological processes.

2.8. Network analysis for the regulated proteins

The proteins of our study were searched against the STRING database version 9 [27] for protein–protein interactions. Only interactions between the proteins belonging to the increased or decreased groups were selected. STRING defines a metric called “confidence score” to define interaction confidence; we fetched all interactions for our regulated dataset which had a confidence score ≥ 0.7 (high confidence). The resulting interactome had 9 nodes and 9 interactions which we named the auditory fear conditioning interaction network (AFCIN) (Fig. 4D).

3. Results

3.1. Auditory fear conditioning induced associative learning

Rats were fear conditioned to a neutral tone and were tested for associative memory retention 24 h later in a distinct context (Fig. 1). Freezing in the fear conditioned group was significantly higher than in the unpaired controls ($n = 5$ for each group, $p < 0.0001$, unpaired t -test). A separate group of animals underwent identical fear conditioning protocol and were sacrificed for tissue harvest without retention tests. Importantly, this protocol has been shown to induce a ~ 2 -fold potentiation of thalamic and cortical input synapses to the lateral amygdala [19,20].

Table 1
Upregulated proteins 24 h after auditory fear conditioning.

IPI	Gene symbol	Average fold change (FC/N)	IPI	Gene symbol	Average fold change (FC/N)
IPI00382186	LOC307347	1.71	IPI00361686	C1qbp	1.15
IPI00366836	Sptbn4	1.52	IPI00204993	Vasn	1.15
IPI00193173	Pcp4	1.44	IPI00869675	Capza1	1.15
IPI00366785	Yars	1.41	IPI00201060	Lmna	1.14
IPI00371167	Pgm2l1	1.32	IPI00207308	Cltb	1.13
IPI00202725	Rps21	1.27	IPI00766788	Oxct1	1.13
IPI00231643	Sod1	1.26	IPI00365600	Prkar2b	1.13
IPI00557154	RGD1560691	1.23	IPI00188732	Syng1	1.13
IPI00230941	Vim	1.22	IPI00190100	S1pr2	1.13
IPI00558765	Clec2d1l	1.21	IPI00205493	Snc	1.13
IPI00187628	Sptb	1.21	IPI00214448	Crym	1.13
IPI00777133	–	1.18	IPI00231067	Vdac3	1.13
IPI00190943	Gfap	1.18	IPI00569785	–	1.12
IPI00210119	Map6	1.18	IPI00395285	Rpl3	1.12
IPI00369394	Nlr1	1.18	IPI00198620	Atp5d	1.12
IPI00231445	Rpl15	1.17	IPI00331865	Dbnl	1.12
IPI00369362	Rtl1	1.16	IPI00325138	Ptprz1	1.12
IPI00869806	Actr1a	1.16	IPI00211864	Sncb	1.12
IPI00373024	Cadm2	1.16	IPI00230793	Plec1	1.12
IPI00231697	Stmn1	1.15	IPI00199600	Atp6v1g1	1.12
IPI00388169	Ccdc110	1.15	IPI00326433	Hspe1	1.11
IPI00567786	–	1.15			

Bold items are proteins that are also strongly upregulated compared to unpaired controls.

3.2. Quantification of proteomic changes in the lateral amygdala upon fear conditioning

The lateral amygdala from six individual sets of fear conditioned rats and naïve/unpaired controls were dissected and labeled with TMT isobaric tags separately for quantitative proteomic analysis. A total of 482 proteins were identified and quantified across all 3 LC-MS/MS runs and 6 biological repetitions. The proteins that were strongly upregulated (43 proteins) or downregulated (20 proteins) in fear conditioned samples are listed in Tables 1 and 2. Intriguingly, seven of the regulated proteins (Gfap, Map6, Pcp4, Snc, Sod1, Syng1, Vdac3) have been previously implicated in LTP, and five (Pcp4, Prkar2b, Snc, Vdac3, Ckb) in learning and memory. Five proteins (Yars, Vim, Oxct1, Crym, Vdac3) that were upregulated after fear conditioning compared to naïve controls were also increased compared to unpaired controls.

The MS/MS spectra for two representative peptides of Vim (Vimentin) are shown in Fig. 2A and B, where the level of mass tags labeling of the fear conditioned group (128, 131) is significantly higher than naïve (126, 129) and unpaired control levels (127, 130). Vimentin has also been reported to show strongly increased mRNA levels after fear conditioning with both microarray and real-time RT-PCR [15], validating the results of our quantitative analysis.

To discern changes in protein expression specifically due to associative learning, we grouped upregulated (Fig. 3A) and downregulated (Fig. 3B) proteins. The strongly regulated proteins in each comparison pair (FC vs. Naïve, Unpaired vs. Naïve, FC vs. Unpaired)

Table 2
Downregulated proteins 24 h after auditory fear conditioning.

IPI	Gene symbol	Average fold change (FC/N)	IPI	Gene symbol	Average fold change (FC/N)
IPI00206226	Cap2	0.94	IPI00192409	Gapdhs	0.93
IPI00213663	Slc1a2	0.94	IPI00198717	Mdh1	0.92
IPI00372080	Sh3glb2	0.94	IPI00558907	LOC363418	0.92
IPI00470288	Ckb	0.94	IPI00231194	Ddah1	0.92
IPI00197555	Suc1g1	0.94	IPI00422092	Rac1	0.92
IPI00362927	Tuba4a	0.94	IPI00191737	Alb	0.90
IPI00364780	Atp6v1h	0.94	IPI00363265	Hspa9	0.89
IPI00231146	Hint1	0.93	IPI00366048	RGD1564195	0.88
IPI00554244	Ampd2	0.93	IPI00568249	–	0.88
IPI00372910	RGD1560402	0.93	IPI00231801	Cst3	0.76

Bold items are proteins that are also strongly downregulated compared to unpaired controls.

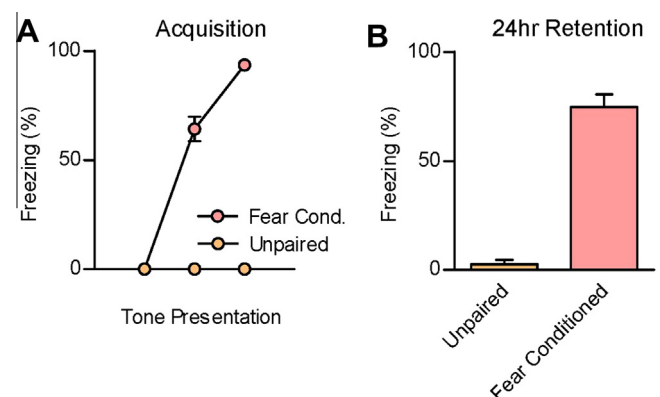


Fig. 1. Auditory fear conditioning induced robust associative learning. (A) Freezing during acquisition. (B) Freezing at retention test 24 h post-conditioning.

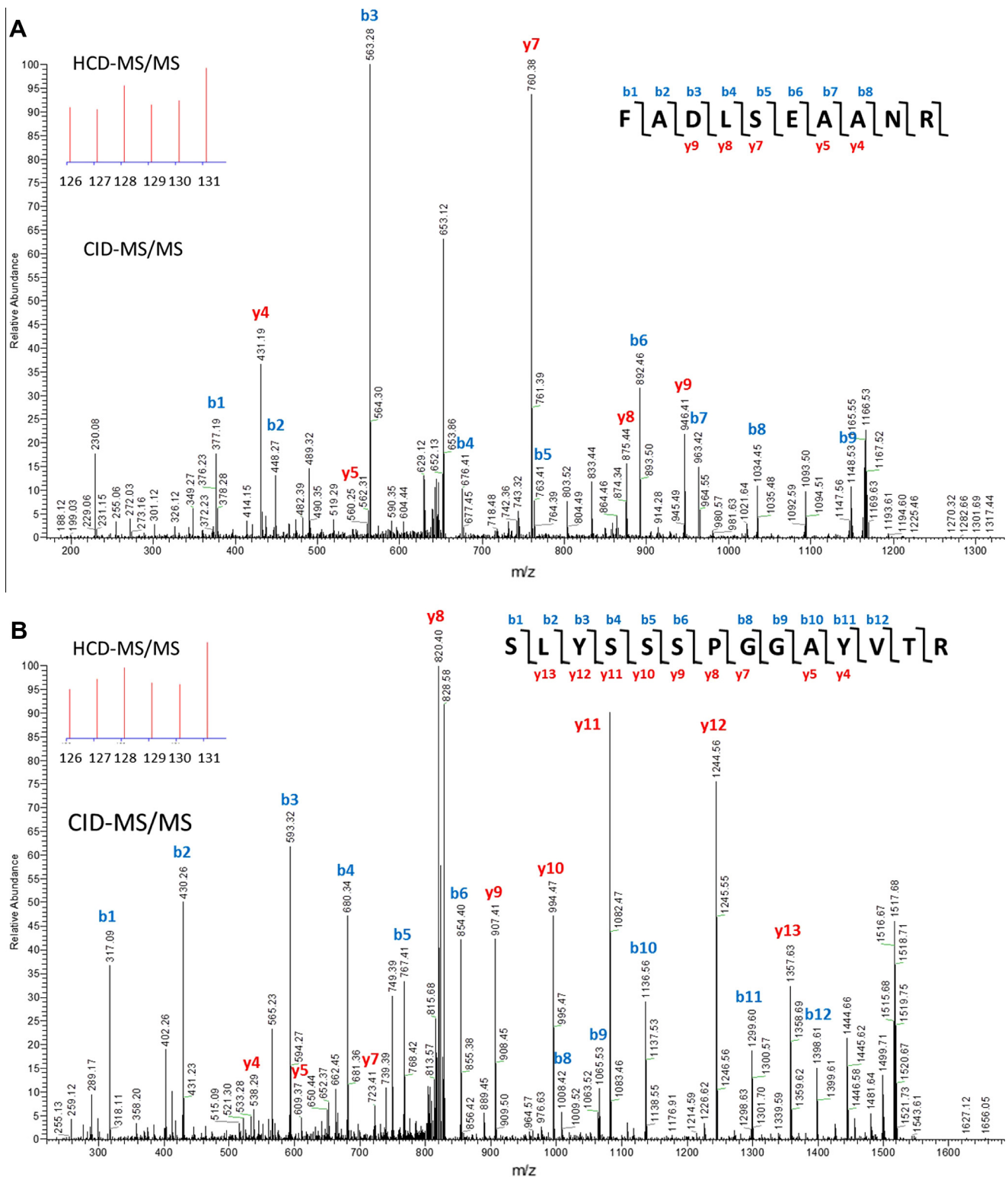


Fig. 2. The CID and HCD MS/MS spectrum of two representative peptides of Vimentin. The peaks in CID reveal precursor peptide sequence based on fragmentation patterns and the HCD MS/MS spectrum detects reporter ions of m/z 126 to 131, used for quantification of the precursor peptide. (A) Tandem MS spectra of peptide FADLSEAA[AN]R from Vimentin. Note that the HCD shows increases in fear conditioned samples (labeled 128, 131) compared to naïve (126, 129) and unpaired controls (127, 130). (B) Tandem MS spectra of peptide SLYSSPGGAYV[TV]R of Vimentin, also increased in fear conditioned samples.

were grouped in three-way Venn diagrams. The proteins that increased (or decreased) in the fear conditioned group but not in the unpaired group are specific to the memory association, suggesting that expression of these proteins may contribute to the cellular/synaptic modifications required to store fear memory.

3.3. Functional annotation of proteins regulated by auditory fear conditioning

The functional annotation of proteins increased or decreased by fear conditioning compared to naïve controls was performed using

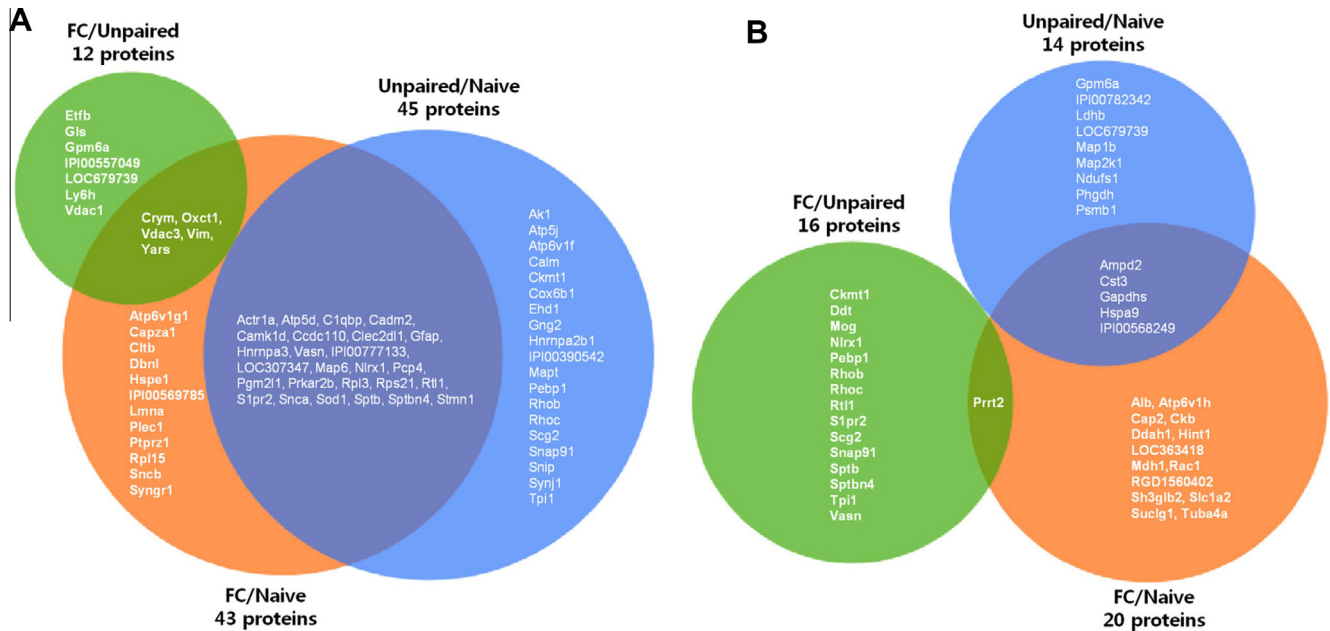


Fig. 3. Differential regulation of protein expression in the lateral amygdala of fear conditioned rats and naïve or unpaired controls. (A) Proteins which showed increased expression in the fear conditioned group compared to the naïve or unpaired group, or in the unpaired group compared to the naïve group are shown in three-way Venn diagrams. Note that proteins increased in the fear conditioned group compared to both naïve and unpaired groups and not in unpaired group compared to naïve group may be considered as proteins that selectively increased upon association (i.e. 'memory proteins'). (B) Proteins which showed decreased expression in the fear conditioned group compared to the naïve or unpaired group, or in the unpaired group compared to the naïve group.

Table 3

Auditory fear conditioning-regulated molecules implicated in the nervous system and behavior.

Functional annotation	p-Value	# of Molecules	Molecules
<i>Nervous system development and function</i>			
Activation of astrocytes	8.14E–06	4	Alb, Gfap, Snca, Vim
Long-term potentiation	1.42E–05	7	Gfap, Map6, Pcp4, Snca, Sod1, Syng1, Vdac3
Motor function	1.68E–05	5	Prkar2b, Rac1, Snca, Snca, Sod1
Activation of neuroglia	2.03E–05	5	Alb, Gfap, Snca, Sod1, Vim
Quantity of neurites	5.80E–05	4	Ptprz1, Rac1, Snca, Snca
Loss of hippocampal neurons	9.70E–05	2	Cst3, Slc1a2
Abnormal morphology of axons	1.34E–04	4	Ckb, Lmna, Plec, Sptbn4
Morphology of nervous system	1.51E–04	11	Ckb, Gfap, Lmna, Plec, Ptprz1, Slc1a2, Snca, Snca, Sod1, Sptbn4, Stmn1
Myelination	1.82E–04	5	Gfap, Lmna, Ptprz1, Rac1, Sptbn4
Morphology of neurites	2.44E–04	5	Ckb, Lmna, Plec, Snca, Sptbn4
Formation of neurites	2.91E–04	5	Camk1d, Ddah1, Map6, Rac1, Snca
Synaptic transmission of synapse	3.82E–04	3	Snca, Snca, Vdac3
Neuritogenesis	1.09E–03	7	Camk1d, Ptprz1, Rac1, S1pr2, Snca, Sptbn4, Stmn1
Outgrowth of axons	2.33E–03	6	Gfap, Ptprz1, Rac1, Sod1, Syng1, Vim
Paired-pulse facilitation of synapse	8.49E–03	2	Syng1, Vdac3
<i>Behavior</i>			
Behavior	2.22E–05	13	Ckb, Dbnl, Gfap, Map6, Pcp4, Prkar2b, Rac1, S1pr2, Slca2, Snca, Sod1, Sptbn4, Vdac3
Swimming behavior	8.20E–05	3	Dbnl, S1pr2, Sod1
Walking	7.75E–03	2	Sod1, Sptbn4
Learning	8.50E–03	5	Ckb, Pcp4, Prkar2b, Snca, Vdac4

Ingenuity Pathway Analysis (IPA). The significance of the functional annotation was determined with *p*-values (as an index of the confidence in the overlap). Functional annotation indicated that 28 of the 63 regulated proteins were involved in nervous system development and function, 13 in animal behavior, and 11 in skeletal & muscular system development and function. The implicated sub-processes of nervous system and behavior are listed in Table 3. As noted previously, various proteins involved in LTP and learning were functionally annotated with high overlap, suggesting their contribution to auditory fear conditioning. Additionally, proteins involved in axon/dendrite development and synaptic transmission contributed a significant portion of the regulated proteins.

3.4. Enrichment analysis of proteins regulated in auditory fear conditioning

We used DAVID to functionally categorize the proteins regulated in auditory fear conditioning by biological process, cellular component, and molecular function (Fig. 4). The results for biological process showed strong enrichment of behavior, cytoskeleton or membrane reorganization, and oxidative stress-related proteins (Fig. 4A). Cellular component analysis showed strong enrichment of axon, cytoskeleton, membrane, and mitochondrial proteins (Fig. 4B). Molecular function annotation revealed enrichment of structural, cytoskeletal, and active transmembrane transporter activity-related proteins (Fig. 4C).

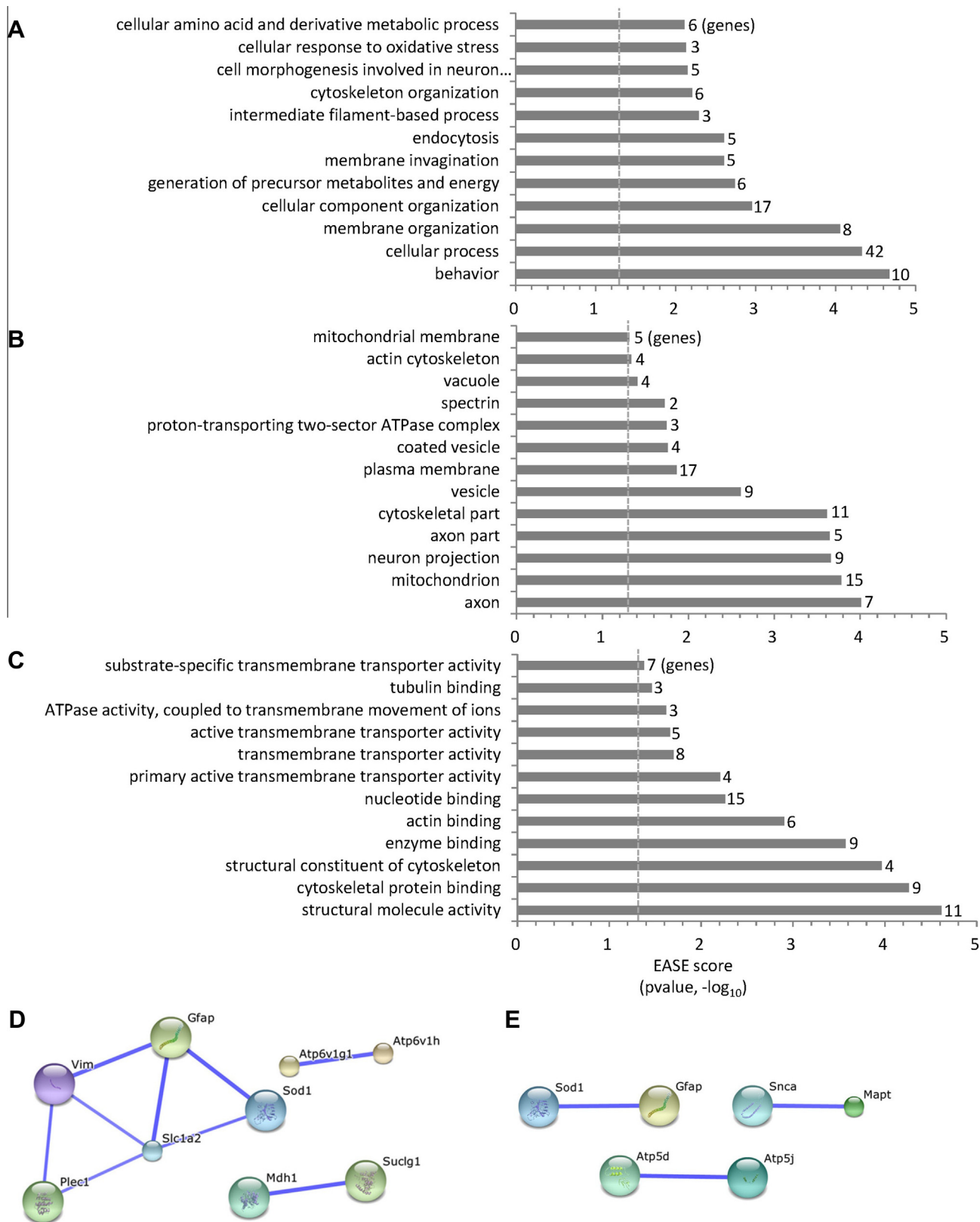


Fig. 4. DAVID Gene Ontology enrichment analysis and STRING analysis of proteins increased and decreased upon auditory fear conditioning in the lateral amygdala. (A) Enrichment analysis by biological process. (B) Enrichment analysis by cellular component (C) Enrichment analysis by molecular function. (D) The auditory fear conditioning interaction network (AFCIN) shows a tightly connected protein–protein interaction network among regulated proteins in the lateral amygdala. Protein interactions among proteins regulated after fear conditioning compared to naïve controls. (E) Protein interactions among proteins regulated after unpairing compared to naïve controls.

3.5. Interaction network analysis of proteins regulated by fear conditioning and unpairing

To identify protein–protein interaction networks among regulated proteins, we employed STRING (Search Tool for the Retrieval of Interacting Genes/Proteins) analysis [27] for proteins that were upregulated or downregulated by fear conditioning or unpairing. In the STRING-generated protein–protein network that we named the auditory fear conditioning interaction network (AFCIN, Fig 4D), several proteins of mainly axonal/dendritic or glial/astrocytic origin, *Plec1*, *Slc1a2*, *Vim*, *Sod1* and *Gfap* constituted a prominent, tightly connected cluster, suggesting coordinated endogenous activity. Other less interconnected interactions were also identified in fear conditioning and unpairing-regulated proteins (Fig. 4E).

4. Discussion

Here we employed quantitative proteomics to examine the expression of hundreds of proteins in the lateral amygdala in response to auditory fear conditioning. We found that various proteins involved in LTP and learning were regulated by fear conditioning. Likewise, large proportions of proteins regulated upon fear conditioning were involved in axon/dendrite growth and development (Table 3). A substantial number of proteins that were upregulated or downregulated by fear conditioning have not yet been studied specifically in learning or synaptic plasticity, warranting further targeted research.

Learning and the subsequent storage of associations in the brain are known to require plasticity at synapses and throughout the neuron. Auditory fear conditioning has been shown to require LTP at input synapses to the basolateral amygdala [10–12]. Accordingly, we found that seven of the regulated proteins (*Gfap* [28], *Map6* [29], *Pcp4* [30], *Snca* [31], *Sod1* [32], *Syng1* [33], *Vdac3* [34]) have been previously implicated in LTP, and five (*Pcp4* [30], *Prkar2b* [35], *Snca* [36], *Vdac3* [34], *Ckb* [37]) in learning and memory. We briefly review the literature for these individual molecules and their role in learning and memory (Supplementary Text).

The fear conditioning interaction network (Fig. 4A) showed a tightly connected cluster of *Plec1*, *Slc1a2*, *Vim*, *Sod1* and *Gfap*. *Slc1a2* is a membrane-bound protein and functions as the principal transporter to clear glutamate from the extracellular space at excitatory synapses [38]. *Vim*, *Plec1* and *Gfap* are all cytoskeletal elements that might have concerted structural effects during the encoding of fear memory. *Slc1a2*, *Sod1* and *Gfap* have prominent roles in glial cells and astrocytes [39,40], suggesting a coordinated endogenous role in auditory fear conditioning.

Although several studies have examined genome-wide mRNA expression after fear conditioning [13–15], this study extends these observations to the protein level. This approach has the advantage of providing a non-biased proteome-wide illustration of the biochemical changes upon learning. Our study may serve as a blueprint in revealing the whole palette of biological processes that mark the engram.

Acknowledgments

This work was supported by National Research Foundation of Korea (NRF) grants (2011-0019226 and 2011-0018209) and by a Korea Basic Science Institute grant (T33615 to YMP, KHK, and SWC). I.H. was supported by NRF grant # 2012R1A6A3A01019438. S.P., J.K., B.A. and S.S. were supported by BK21 Research Fellowships from the Korea Ministry of Education.

Appendix A. Supplementary data

Supplementary data associated with this article can be found, in the online version, at <http://dx.doi.org/10.1016/j.bbrc.2013.03.060>.

References

- [1] E.R. Kandel, The molecular biology of memory storage: a dialogue between genes and synapses, *Science* 294 (2001) 1030–1038.
- [2] J.L. McGaugh, Memory—A century of consolidation, *Science* 287 (2000) 248–251.
- [3] P.W. Frankland, B. Bontempi, The role of the amygdala in fear and anxiety, *Nature Reviews of Neuroscience* 6 (2005) 119–130.
- [4] M. Davis, The role of the amygdala in fear and anxiety, *Annual Review of Neuroscience* 15 (1992) 353–375.
- [5] J.E. LeDoux, Emotion circuits in the brain, *Annual Review of Neuroscience* 23 (2000) 155–184.
- [6] J.P. Johansen, C.K. Cain, L.E. Ostroff, J.E. LeDoux, Molecular mechanisms of fear learning and memory, *Cell* 147 (2011) 509–524.
- [7] I. Hong, J. Kim, B. Song, S. Park, J. Lee, J. Kim, B. An, S. Lee, S. Choi, Modulation of fear memory by retrieval and extinction: a clue for memory deconsolidation, *Reviews in the Neurosciences* 22 (2011) 205–229.
- [8] M.T. Rogan, U.V. Staubli, J.E. LeDoux, Fear conditioning induces associative long-term potentiation in the amygdala, *Nature* 390 (1997) 604–607.
- [9] M.G. McKernan, P. Shinnick-Gallagher, Fear conditioning induces a lasting potentiation of synaptic currents in vitro, *Nature* 390 (1997) 607–611.
- [10] S. Rumpel, J. LeDoux, A. Zador, R. Malinow, Postsynaptic receptor trafficking underlying a form of associative learning, *Science* 308 (2005) 83–88.
- [11] M.J. Miserendino, C.B. Sananes, K.R. Melia, M. Davis, Blocking of acquisition but not expression of conditioned fear-potentiated startle by NMDA antagonists in the amygdala, *Nature* 345 (1990) 716–718.
- [12] M.S. Fanselow, J.J. Kim, Acquisition of contextual Pavlovian fear conditioning is blocked by application of an NMDA receptor antagonist D, L-2-amino-5-phosphonopentanoic acid to the basolateral amygdala, *Behavioral Neuroscience* 108 (1994) 210–212.
- [13] R. Lamprecht, S. Dracheva, S. Assoun, J.E. LeDoux, Fear conditioning induces distinct patterns of gene expression in lateral amygdala, *Genes, Brain and Behavior* 8 (2009) 735–743.
- [14] J.E. Ploski, K.W. Park, J. Ping, M.S. Monsey, G.E. Schafe, Identification of plasticity-associated genes regulated by Pavlovian fear conditioning in the lateral amygdala, *Journal of Neurochemistry* 112 (2010) 636–650.
- [15] B. Mei, C. Li, S. Dong, C. Jiang, H. Wang, Y. Hu, Distinct gene expression profiles in hippocampus and amygdala after fear conditioning, *Brain Research Bulletin* 67 (2005) 1–12.
- [16] M. Bantscheff, M. Schirle, G. Sweetman, J. Rick, B. Kuster, Quantitative mass spectrometry in proteomics: a critical review, *Analytical and Bioanalytical Chemistry* 389 (2007) 1017–1031.
- [17] B. Domon, R. Aebersold, Options and considerations when selecting a quantitative proteomics strategy, *Nature Biotechnology* 28 (2010) 710–721.
- [18] J. Cox, M. Mann, Quantitative, high-resolution proteomics for data-driven systems biology, *Annual Review of Biochemistry* 80 (2011) 273–299.
- [19] J. Kim, S. Lee, K. Park, I. Hong, B. Song, G. Son, H. Park, W.R. Kim, E. Park, H.K. Choe, H. Kim, C. Lee, W. Sun, K. Kim, K.S. Shin, S. Choi, Amygdala depotentiation and fear extinction, *Proceedings of the National Academy of Sciences of the United States of America* 104 (2007) 20955–20960.
- [20] I. Hong, B. Song, S. Lee, J. Kim, S. Choi, Extinction of cued fear memory involves a distinct form of depotentiation at cortical input synapses onto the lateral amygdala, *European Journal of Neuroscience* 30 (2009) 2089–2099.
- [21] I. Hong, J. Kim, J. Lee, S. Park, B. Song, J. Kim, B. An, K. Park, H.W. Lee, S. Lee, H. Kim, S.H. Park, K.D. Eom, S. Lee, S. Choi, Reversible plasticity of fear memory-encoding amygdala synaptic circuits even after fear memory consolidation, *PLoS ONE* 6 (2011) e24260.
- [22] I. Hong, J. Kim, B. Song, K. Park, K. Shin, K.D. Eom, P.L. Han, S. Lee, S. Choi, Fear conditioning occludes late-phase long-term potentiation at thalamic input synapses onto the lateral amygdala in rat brain slices, *Neuroscience Letters* 506 (2012) 121–125.
- [23] M.P. Washburn, D. Wolters, J.R. Yates 3rd, Large-scale analysis of the yeast proteome by multidimensional protein identification technology, *Nature Biotechnology* 19 (2001) 242–247.
- [24] K. Byun, J. Young Kim, E. Bayarsaikhan, D. Kim, G.B. Jeong, K.N. Yun, H. Kyeong Min, S.U. Kim, J.S. Yoo, B. Lee, Quantitative proteomic analysis reveals that lipopolysaccharide induces mitogen-activated protein kinase-dependent activation in human microglial cells, *Electrophoresis* 33 (2012) 3756–3763.
- [25] C. Raso, C. Cosentino, M. Gaspari, N. Malara, X. Han, D. McClatchy, S.K. Park, M. Renne, N. Vadalà, U. Prati, G. Cuda, V. Mollace, F. Amato, J.R. Yates 3rd, Characterization of breast cancer interstitial fluids by TmT labeling LTQ-orbitrap mass spectrometry and pathway analysis, *Journal of Proteome Research* (2012).
- [26] D.W. Huang, B.T. Sherman, R.A. Lempicki, Systematic and integrative analysis of large gene lists using DAVID bioinformatics resources, *Nature Protocols* 4 (2009) 44–57.
- [27] D. Szklarczyk, A. Franceschini, M. Kuhn, M. Simonovic, A. Roth, P. Minguet, T. Doerks, M. Stark, J. Muller, P. Bork, L.J. Jensen, C. von Mering, The STRING

- database in 2011: functional interaction networks of proteins, globally integrated and scored, *Nucleic Acids Research* 39 (2011) D561–D568.
- [28] M.A. McCall, R.G. Gregg, R.R. Behringer, M. Brenner, C.L. Delaney, E.J. Galbreath, C.L. Zhang, R.A. Pearce, S.Y. Chiu, A. Messing, Targeted deletion in astrocyte intermediate filament (Gfap) alters neuronal physiology, *Proceedings of the National Academy of Sciences of the United States of America* 93 (1996) 6361–6366.
- [29] J. Volle, J. Brocard, M. Saoud, S. Gory-Faure, J. Brunelin, A. Andrieux, M.F. Suaud-Chagny, Reduced expression of STOP/MAP6 in mice leads to cognitive deficits, *Schizophrenia Bulletin* (2012).
- [30] P. Wei, J.A. Blundon, Y. Rong, S.S. Zakharenko, J.I. Morgan, Impaired locomotor learning and altered cerebellar synaptic plasticity in pep-19/PCP4-null mice, *Molecular and Cellular Biology* 31 (2011) 2838–2844.
- [31] S. Liu, I. Ninan, I. Antonova, F. Battaglia, F. Trinchese, A. Narasanna, N. Kolodilov, W. Dauer, R.D. Hawkins, O. Arancio, Alpha-Synuclein produces a long-lasting increase in neurotransmitter release, *EMBO Journal* 23 (2004) 4506–4516.
- [32] E. Klann, E.D. Roberson, L.T. Knapp, J.D. Sweatt, A role for superoxide in protein kinase C activation and induction of long-term potentiation, *Journal of Biological Chemistry* 273 (1998) 4516–4522.
- [33] R. Janz, T.C. Sudhof, R.E. Hammer, V. Unni, S.A. Siegelbaum, V.Y. Bolshakov, Essential roles in synaptic plasticity for synaptogyrin I and synaptophysin I, *Neuron* 24 (1999) 687–700.
- [34] E.J. Weeber, M. Levy, M.J. Sampson, K. Anflous, D.L. Armstrong, S.E. Brown, J.D. Sweatt, W.J. Craigen, The role of mitochondrial porins and the permeability transition pore in learning and synaptic plasticity, *Journal of Biological Chemistry* 277 (2002) 18891–18897.
- [35] E.P. Brandon, S.F. Logue, M.R. Adams, M. Qi, S.P. Sullivan, A.M. Matsumoto, D.M. Dorsa, J.M. Wehner, G.S. McKnight, R.L. Idzerda, Defective motor behavior and neural gene expression in Rllbeta-protein kinase A mutant mice, *Journal of Neuroscience* 18 (1998) 3639–3649.
- [36] Y. Lim, V.M. Kehm, E.B. Lee, J.H. Soper, C. Li, J.Q. Trojanowski, V.M. Lee, Alpha-Syn suppression reverses synaptic and memory defects in a mouse model of dementia with Lewy bodies, *Journal of Neuroscience* 31 (2011) 10076–10087.
- [37] C.R. Jost, C.E. Van Der Zee, H.J. In 't Zandt, F. Oerlemans, M. Verheij, F. Streijger, J. Fransen, A. Heerschap, A.R. Cools, B. Wieringa, Creatine kinase B-driven energy transfer in the brain is important for habituation and spatial learning behaviour, mossy fibre field size and determination of seizure susceptibility, *European Journal of Neuroscience* 15 (2002) 1692–1706.
- [38] Y. Kanai, M.A. Hediger, The glutamate/neutral amino acid transporter family SLC1: molecular, physiological and pharmacological aspects, *Pflügers Archiv-European Journal of Physiology* 447 (2004) 469–479.
- [39] C.M. Anderson, R.A. Swanson, Astrocyte glutamate transport: review of properties, regulation, and physiological functions, *Glia* 32 (2000) 1–14.
- [40] A.M. Clement, M.D. Nguyen, E.A. Roberts, M.L. Garcia, S. Boillee, M. Rule, A.P. McMahon, W. Doucette, D. Siwek, R.J. Ferrante, R.H. Brown Jr., J.P. Julien, L.S. Goldstein, D.W. Cleveland, Wild-type nonneuronal cells extend survival of SOD1 mutant motor neurons in ALS mice, *Science* 302 (2003) 113–117.